

Violation of local realism in a high-dimensional two-photon setup with non-integer spiral phase plates

S.S.R. Oemrawsingh, A. Aiello, E.R. Eliel, and J.P. Woerdman
 Huygens Laboratory, Leiden University
 P.O. Box 9504, 2300 RA Leiden, The Netherlands

We propose a novel setup to investigate the quantum non-locality of orbital angular momentum states living in a high-dimensional Hilbert space. We incorporate non-integer spiral phase plates in spatial analyzers, enabling us to use only two detectors. The resulting setup is somewhat reminiscent of that used to measure polarization entanglement. However, the two-photon states that are produced, are not confined to a 2 × 2-dimensional Hilbert space, and the setup allows the probing of correlations in a high-dimensional space. For the special case of half-integer spiral phase plates, we predict a violation of the Clauser-Horne-Shimony-Holt version of the Bell inequality ($S > 2$), that is even stronger than achievable for two qubits ($S = 2\sqrt{2}$), namely $S = 3\frac{1}{5}$.

PACS numbers: 03.67.Mn, 42.50.Dv

I. INTRODUCTION

Recently, the orbital angular momentum (OAM) of light has drawn considerable interest in the context of quantum information processing. The spatial degrees of freedom involved in OAM [1] provide a high-dimensional alphabet to quantum information processing (i.e. qunits instead of qubits) [2, 3]. Additionally, since OAM is associated with the topology of the electromagnetic field, the use of this observable in quantum entanglement may lead to states that are inherently robust against decoherence [4].

The most popular OAM analyzer when dealing with conservation, correlation and entanglement of OAM consists of a so-called fork hologram [5], i.e. a binary phase hologram containing a fork in its center [6], together with a spatial mode detector consisting of a single-mode fiber connected to a single-photon detector; such analyzers have been used in the three-dimensional case, i.e. $N = 3$, by Vaziri et al., [3]. In that experiment, proof of entanglement of the OAM degree of freedom of two photons was given by showing that a generalized Bell inequality was violated; this scheme requires 6 detectors, namely 3 in each arm, and one has to measure 3 × 3 coincidence count rates [3] to perform a measurement for a single setting of the analyzers.

In the present paper, we consider the use of spiral phase plates (SPPs) [7] instead of phase holograms in an OAM entanglement setup, enabling us to investigate high-dimensional entanglement with only two detectors. More specifically, we will consider SPPs that impose on an optical beam a non-integer OAM expectation value per photon, in units of \hbar [7]. With such devices, combined with single-mode fibers to form quantum-state analyzers, we propose to build an OAM entanglement setup that is reminiscent of the usual setup to measure polarization entanglement [8], where the rotational settings of the analyzers (polarizers in that case) is varied. We will show that it is possible to identify SPP analyzer settings, in the spirit of horizontal and vertical aligned polarizers, when

using half-integer SPPs, allowing observation of high-dimensional entanglement ($N > 2$), in contrast to the polarization case ($N = 2$). These claims are supported by quantitative calculations; we predict highly non-classical quantum correlations ($S = 3\frac{1}{5}$), i.e. stronger quantum correlation between two photons than the maximum correlation between two qubits ($S = 2\sqrt{2}$).

II. SPIRAL PHASE PLATES

A SPP, shown in Fig. 1(a), is a transparent dielectric plate with a thickness that varies as a smooth ramp, thus phase shifting an incident field linearly with the azimuthal angle [7]. As can be seen, the plate carries a screw discontinuity, expressed by the spiraling thickness, and an edge discontinuity, i.e. the radial step with height h_s . The difference between the maximum and minimum phase shift is written as $2\pi\ell$, where ℓ is not necessarily integer; in fact, ℓ depends on the step height h_s , the difference in refractive indices of the SPP and surrounding medium, and the wavelength of the incident light [7]. Thus, a photon propagating through this plate will acquire an OAM with expectation value equal to $\ell\hbar$ [7, 9]. Placing such a plate in the waist of Laguerre-Gaussian beam, the field in the exit plane just behind the plate will be described by

$$\langle \ell; \pi | \hat{S}(\ell) | \ell; \pi \rangle = u_{LG}^{lp}(\mathbf{r}; \ell) \exp(i\ell\phi); \quad (1)$$

where $|\ell; \pi\rangle$ are the Laguerre-Gaussian (LG) field states and $\hat{S}(\ell)$ is the operator representing the effect of the SPP on the input mode. Note that we have neglected the uniform phase shift that is caused by the SPP's base with height h_0 , since it acts as a plane-parallel plate. By adding another plane-parallel plate with the appropriate thickness, the total phase shift of these two can be made equal to an integer multiple of 2π .

The function $u_{LG}^{lp}(\mathbf{r}; \ell)$ in Eq. (1) is the complex amplitude of the Laguerre-Gaussian beam in its waist plane,

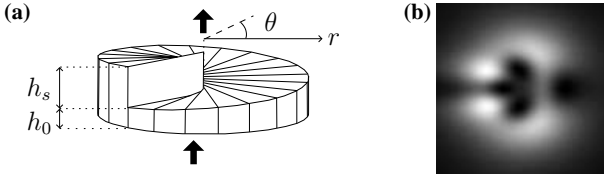


FIG. 1: (a) Schematic drawing of a SPP. The device shifts the phase of an incident beam proportional to the azimuthal angle ϕ . (b) A calculated far-field diffraction pattern of a fundamental Gaussian beam after propagating through an $l = 3\frac{1}{2}$ plate positioned in its waist plane, showing that rotational symmetry is broken. Black and white denote low and high intensity, respectively.

given by [1]

$$\begin{aligned} \text{hr}; \text{pl}; \text{pi} &= u_{lp}^{LG}(r; \phi) \\ &= C_{lp} (1)^p \frac{r^p}{w_0} \frac{L_p^l}{2} \frac{2r^2}{w_0^2} \\ &\exp\left(-\frac{r^2}{w_0^2}\right) \exp(i l \phi); \end{aligned} \quad (2)$$

where w_0 is the waist radius, $L_p^l(x)$ an associated Laguerre polynomial [10] and C_{lp} a normalization constant. In the paraxial limit, the LG free-space modes, enumerated by the (integer) indices l and p , form a complete basis of spatial modes. The LG index l , which should not be confused with the SPP step index l , is related to the OAM that is carried in that LG mode, namely l -per photon [1, 7, 9], while the index p provides information on the number of nodes along a transverse radius of the mode. When placing a SPP in a single LG mode, the output will generally be in a superposition of LG modes and will be no longer invariant under free-space propagation. For integer values of the step index l of the SPP, the edge discontinuity is effectively absent and the superposition will only be with respect to the LG-index p [7, 11]. In that case, the intensity distribution of the mode will be doughnut-shaped in the far field. For non-integer l values, this superposition will also be with respect to the index l , which is related to the OAM of the mode [7]. Such superpositions consist in principle of an infinite number of LG components. Effectively, this number is finite and increases with l ; as an example, if $l = \frac{1}{2}$, 11 LG components are sufficient to describe 87% of the field behind the SPP, while for $l = \frac{5}{2}$, 224 LG components are required. As SPPs with non-integer l can create such high-dimensional superpositions of OAM modes, we anticipate that, when employed suitably, they can also project onto such superpositions. We therefore propose to incorporate such non-integer SPPs in analyzers for OAM states living in a high-dimensional Hilbert space.

From a topological point of view, SPPs with non-integer l imprint a mixed screw-edge dislocation on an incident field. The result is rotational asymmetry of the

imprinted phase distribution and thus of the emerging field, which becomes visible in the far-field intensity profile (Fig. 1 (b)). It is the orientation of the step in the transverse plane, that we wish to exploit as an analyzer setting in a new bipartite entanglement scheme.

Since l shall be chosen to have a non-integer value, it is important to realize that, when an incident field passes through an SPP in combination with its complement (i.e. a SPP with the same step height and orientation, but an inverted vorticity), the beam basically passes through a plane-parallel plate that shifts the phase of the field, in an azimuthally uniform way, by $2\pi l$,

$$\hat{S}^{\text{compl}}(l) \hat{S}(l) = \exp(i2\pi l) \hat{I}; \quad (3)$$

where \hat{I} is the identity operator and where we keep the exponent since $\exp(i2\pi l) \neq 1$ for non-integer l . Since $\hat{S}(l)$ is unitary, it follows that

$$\hat{S}^{\text{compl}}(l) = \exp(i2\pi l) \hat{S}^\dagger(l); \quad (4)$$

where $\hat{S}^\dagger(l)$ is the Hermitian conjugate of $\hat{S}(l)$. As $\hat{S}^\dagger(l)$ and $\hat{S}^{\text{compl}}(l)$ only differ by a multiplicative phase factor we can again use a plane-parallel plate in the experiment to compensate this phase factor. Similar to the uniform phase shift caused by the SPP's base h_0 , we will neglect this phase shift as well, as it can be trivially dealt with. Henceforth, the operator for the compensating SPP, with inverted vorticity, will be represented by the operator $\hat{S}^\dagger(l)$.

III. PROPOSAL FOR AN EXPERIMENT

In the experiment on OAM qutrits ($N = 3$), fork holograms were used [3]. Those holograms can only modify the OAM expectation value by an integer number [12], depending on the diffraction order of the hologram. It also required the use of three analyzers in each arm of a SPDC setup. In contrast, our proposed OAM entanglement experiment uses non-integer SPP state detectors and only requires a single analyzer-detector combination in each arm. This scheme is shown in Fig. 2; it has been inspired by the setup used in polarization entanglement [8]. The SPPs that are inserted in the two arms should be chosen to obey conservation of OAM (see also section VI). Thus, if the classical pump beam does not contain any OAM, a typical choice for the signal and idler SPPs would be to have step indices l and $-l$ respectively, where, in our case, l should have a non-integer value. The role of the lenses in signal and idler path, L_s and L_i respectively, will be discussed in section VI. Finally, single-mode fibers are indicated by F_s and F_i .

By manipulating the transverse axes of our analyzers, namely the step edges, we have access to photon states that live in a high-dimensional OAM Hilbert space, as mentioned earlier. We may orient these edges arbitrarily in the transverse plane, as shown in Fig. 2, thus allowing

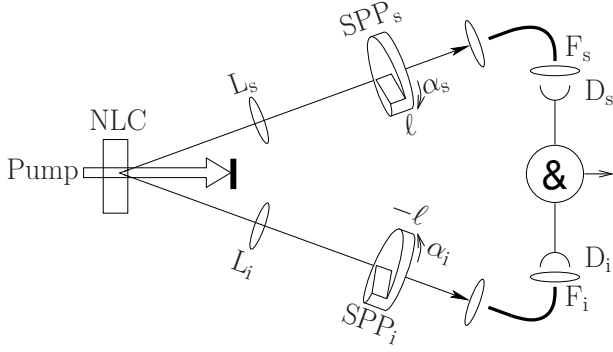


FIG. 2: Proposed experimental setup. A nonlinear crystal (NLC) splits a pump photon in a signal photon and an idler photon by the process of spontaneous parametric down-conversion (SPDC). In each path, a SPP ($SPP_{s,i}$) is inserted with a single-mode fiber $F_{s,i}$, together forming the analyzer. The coincidence count rate of detectors $D_{s,i}$ is measured as a function of the SPP angular settings α_s and α_i .

their use as angular analyzers. When combined with a single-mode fiber, the SPP with step index ℓ , set at an azimuthal angle α_s , projects the incident photon state out onto the OAM state with expectation value ℓ with edge angle α_s . As we will argue in section VI, the coincidence count rate will depend, like in polarization entanglement, only on the relative angle of the transverse axes.

We stress that, in spite of the superficial similarity between a polarizer and a non-integer SPP, they are of course very different devices; for example, while polarization corresponds to alignment, the SPP edge corresponds to orientation. In other words, with a polarizer, one can analyze the alignment of the electrical field oscillation, either horizontal or vertical, thus yielding a periodicity of π when rotated. With a SPP with non-integer ℓ one can analyze the spatial orientation of a field, thus yielding a periodicity of 2π when rotated (see e.g. Fig. 1(b)). Thus we expect that the coincidence count rate will have a periodicity of 2π when one of our analyzers is rotated.

An equally important difference between the two cases is that, whereas polarization Hilbert space is two dimensional, OAM Hilbert space is infinite dimensional. As we will see, this makes rotation of SPPs fundamentally different from rotation of a polarizer. In order to address these aspects explicitly, we need a basis of the OAM Hilbert space that is suited for our purpose.

IV. NON-INTEGER OAM STATES

Our aim is to construct a complete, orthonormal basis that contains non-integer OAM states as basis elements. For that, we need to transform the LG basis. In the polar representation in real space, the LG-basis states are, in their waist plane, given by Eq. (2). These functions can be separated into a radial part $u_{lp}(r)$ and an azimuthal

part $v_l(\theta)$, so that

$$u_{lp}(r) = u_{lp}(r) v_l(\theta); \quad (5)$$

where we can define

$$v_l(\theta) = \sum_j |j\rangle \langle j|; \quad (6)$$

$$u_{lp}(r) = u_{lp}(r) \frac{1}{\sqrt{2}} \exp(i\ell\theta); \quad (7)$$

$$v_l(\theta) = \frac{1}{\sqrt{2}} \exp(i\ell\theta); \quad (8)$$

Here, we have introduced the direction ket $|j\rangle$ and the states $|j\rangle$. The latter, eigenstates of the OAM operator, $\hat{L}_z |j\rangle = \ell |j\rangle$, provide a complete, orthonormal basis for the OAM Hilbert space. The ket $|j\rangle$, which is only valid when using the polar representation, satisfies the orthogonality relation,

$$\int_0^{2\pi} |j\rangle \langle j| = \int_0^{2\pi} |j\rangle \langle j| r dr = \delta_{jj}; \quad (9)$$

We now transform the basis $|j\rangle$ from integer to non-integer OAM. By applying a unitary operator to the integer OAM basis, its completeness and orthonormality are conserved; the unitary operator that we use is the SPP operator, introduced in Eq. (1):

$$|j\rangle \langle j| \rightarrow |j\rangle \langle j| = \frac{1}{\sqrt{2}} \exp(i\ell\theta); \quad (10)$$

The new basis $|j\rangle$ has its components enumerated by ℓ , each with OAM equal to $(\ell + \frac{1}{2})$, where $\frac{1}{2}$ is a constant (not to be confused with the wavelength of the light). Different values of ℓ define different bases of OAM Hilbert space, each basis being complete and orthonormal.

As an example, passing a photon in a fundamental Gaussian mode $|j_{00}\rangle$ through a SPP with $\ell = \frac{2}{3}$, creates the state $|j_{00}\rangle \frac{1}{\sqrt{2}} |j_{2=3}\rangle$; sending this latter photon through a SPP with $\ell = \frac{2}{3}$ (combined with a single-mode fiber) as spatial analyzer then yields a detection probability of unity.

V. ORIENTATION OF THE EDGE DISLOCATION

Since we intend to rotate the non-integer SPPs, it is important to also have a description of the states that arise when the SPP is rotated while the coordinate system is fixed. To gain insight, we show in Fig. 3 the phase shift imposed by a SPP as a function of the azimuthal angle. The solid line represents the imprinted phase for a SPP with its edge oriented at an angle $\alpha = 0$, while the dashed line corresponds to a SPP with edge orientation $\alpha = \pi$. We can now generalize the definition of the

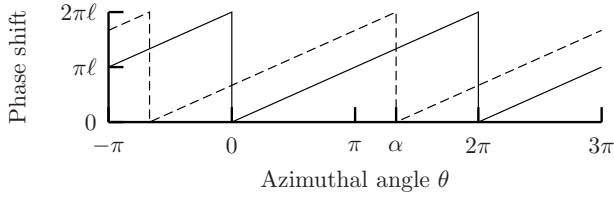


FIG. 3: Plot of the phase shift in printed by a SPP as a function of the azimuthal angle. The solid line shows this shift for a plate with its edge oriented at $= 0$, while the dashed line shows the phase shift for a plate with its edge at $=$.

operator $\hat{S}(\lambda)$ to the operator $\hat{S}(\lambda; \alpha)$, which includes the orientation α of the edge dislocation. We find

$$\langle \mathbf{j} | \hat{S}(\lambda; \alpha) | \mathbf{i} \rangle = \frac{1}{2} \exp[i(1 + \lambda)\alpha] \begin{cases} \exp[i(2\lambda - 1)\alpha]; & 0 < \alpha < \pi; \\ \exp(-i\alpha); & \pi < \alpha < 2\pi; \end{cases} \quad (11)$$

where $\mathbf{j} \in \{0, 2\}$. This also allows us to generalize the states $|\mathbf{j}^{(1)}\rangle$ with orientation $\alpha = 0$ to states with arbitrary orientation, $|\mathbf{j}^{(1)}(\alpha)\rangle$. From Eq. (11), it is immediately clear that, when neglecting the uniform phase shift, the complementary SPP operator $\hat{S}^{\text{comp}}(\lambda; \alpha)$ is equal to $\hat{S}(\lambda; \alpha)^\dagger = \hat{S}(\lambda; \alpha)$.

Since the basis $|\mathbf{j}^{(1)}(0)\rangle$ is complete, the states after rotation, $|\mathbf{j}^{(1)}(\alpha)\rangle$ can be written as a superposition of these basis states. Thus the decomposition of $|\mathbf{j}^{(1)}(\alpha)\rangle$ into the basis $|\mathbf{j}^{(1)}(0)\rangle$ depends on the angle α . To illustrate this, we make a projection of a non-integer state oriented at $\alpha = \lambda$, onto the same state with orientation $\alpha = 0$. For this, we choose a SPP with step $\ell = j + \lambda$, where j is the integer part of the step (not to be confused with the integer LG index l), and $\lambda \in [0; 1)$, yielding the overlap amplitude

$$\begin{aligned} A(\lambda) &= \langle \mathbf{j}^{(1)}(0) | \mathbf{j}^{(1)}(\lambda) \rangle \\ &= \langle \mathbf{j}^{(1)}(0; j + \lambda) | \hat{S}(\lambda; j + \lambda) | \mathbf{j} \rangle \\ &= \frac{1}{2} [2 + \exp(i2\lambda)] \exp(-i(1 + j + \lambda)\alpha); \end{aligned} \quad (12)$$

where $|\mathbf{j} \rangle$ is the angular part of the incident LG state with OAM l . The overlap is then

$$|A(\lambda)|^2 = 1 - \sin^2(\lambda) + \cos^2(\lambda); \quad (13)$$

which depends neither on the integer part of the step index j nor on the OAM state l . For non-zero values of λ , this overlap function has a quadratic dependence on the orientation α . This function is plotted in Fig. 4 for

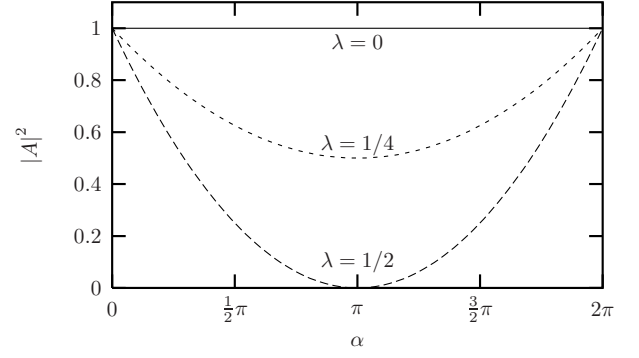


FIG. 4: The overlap (see Eq. (13)) between a non-integer OAM state and the identical state rotated over α . When $\alpha = 0$, the states are identical aside from a trivial phase shift, due to the vanishing edge dislocation. For half-integer OAM, i.e. $\lambda = \frac{1}{2}$, the two states are generally different, leading to a parabolic dependence of their overlap; the two states are orthogonal when $\alpha = \pi$.

various values of λ . It illustrates that, when $\alpha = 0$, the projection does not change, as expected. For values of $\lambda \notin \{0\}$, the outcome of the projection is less trivial, with $\lambda = \frac{1}{2}$ providing an especially interesting case: when the state is rotated over $\alpha = \pi$ by rotating the SPP, the state is orthogonal to the non-rotated state. We will call the half-integer states $|\mathbf{j}^{(1)}(0)\rangle$ and $|\mathbf{j}^{(1)}(\pi)\rangle$ 'up' and 'down', respectively, referring to the orientation of the edge part of the dislocation. In principle, this orientational label can be used for any non-integer OAM state, but for half-integer OAM states it carries an analogy to fermionic spin, as our 'up' and 'down' states are orthogonal just like up and down spin $\frac{1}{2}$. In polarization entanglement the comparable orientational labels are known as H' for horizontal and V' for vertical polarization. To make our proposed OAM entanglement setup maximally equivalent to the polarizer setup, we focus from now on mainly on the case $\lambda = \frac{1}{2}$. Note that, as Eq. (13) is independent of j , any SPP with $\ell = j + \lambda$ may be used, as long as $\lambda = \frac{1}{2}$.

There is, however, a key difference between the half-integer OAM states on the one hand and the fermionic spin states or polarization states on the other hand. Angularly intermediate states of the fermionic spin or of polarization are a superposition of the two orthogonal basis states 'up' and 'down', or H' and V', so that the overlap function varies as $\sin^2(\alpha)$. However, from Eq. (13) we see that in the present case, the dependence of $|A|^2$ on α yields a parabola. Thus we conclude that, as the SPP is rotated from 'up' to 'down', the OAM state follows a path through Hilbert space that is not confined to the two-dimensional subspace spanned by the 'up' and 'down' states. Note that the OAM expectation value will be conserved along this path, as rotating the SPP has, of course, no effect on its step height, i.e. on ℓ .

VI. ENTANGLEMENT OF HALF-INTEGER ORBITAL ANGULAR MOMENTUM STATES

Entanglement issues in a setup as in Fig. 2 are conveniently described by the "advanced-wave" theory introduced by Klyshko et al. as a model for two-photon optics [13]. This theory is based on a Green's function approach in which, due to conservation laws, the nonlinear crystal when pumped by a laser beam, can be treated as a "geometrical-optics reflection" mirror for the advanced wave, thus fixing possible paths for the signal and idler photons in the experiment. The conservation laws are a consequence of the (nonlinear) SPDC process; they are the only remnant of the crystal nonlinearity in Klyshko's theory, which, otherwise, is a purely linear theory. In this way, the pump-beam parameters set the mirror's size and curvature. In a crude way, one can think of the experiment as sending photons from the signal detector via the mirror towards the idler detector. Thus the setting of an element in the signal path influences what happens in the idler path.

The conservation law that we need specifically is that of conservation of OAM in SPDC. This issue has been discussed in several recent papers [2, 14, 15, 16, 17, 18, 19] and it seems that OAM is indeed conserved if two conditions are fulfilled, namely (i) the paraxial limit, and (ii) the thin-crystal limit. In practice this is usually the case.

The SPPs are linear-optics devices, so that the advanced-wave theory should be valid. The lenses indicated by L_s and L_i in Fig. 2, image the SPP in the signal path via the effective mirror onto the SPP in the idler path. The positioning of L_s and L_i depends on the curvature of the mirror, i.e. on the wavefront curvature of the pump beam. For the simplest case where the pump beam is a plane wave, the effective mirror is planar, as shown in the setup of Fig. 5. Any image inversion caused by the imaging is not taken into account below, in order not to complicate the discussion. Finally, we assume that when a pump beam contains OAM due to an exponential phase factor, it can be replaced, in this model, by an element that lets the signal photon state gain exactly that amount of OAM after reflection, so that the conservation laws in SPDC [2, 14, 15, 16, 17, 18, 19] are obeyed.

When choosing a fundamental Gaussian pump beam and accounting for OAM conservation, the two-photon state can be described in the LG basis as

$$|j\rangle_i = \sum_{l;p;p^0} C_{l;p;p^0} |j;p;j\rangle_l |p^0\rangle_i \quad (14)$$

where $C_{l;p;p^0}$ are relative weights given by

$$C_{l;p;p^0} = h_{\text{pump}} |j\rangle_l |p\rangle_i |p^0\rangle_i; \quad (15)$$

where \hat{h} represents the crystal's action and $|j\rangle_{\text{pump}}$ is the state of the pump photon. As stated before, we restrict ourselves to a pump state $|j\rangle_i$ and half-integer SPPs,

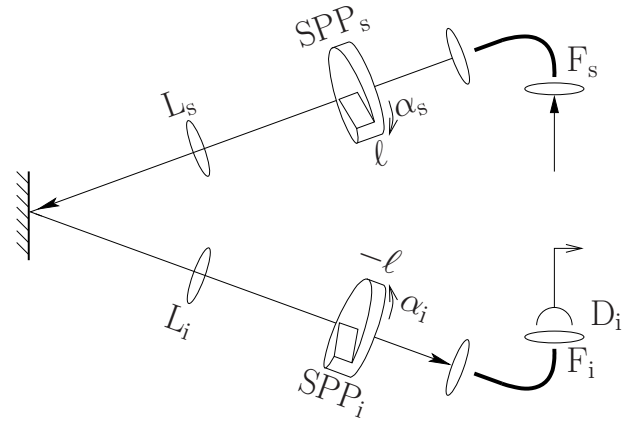


FIG. 5: According to the advanced-wave theory of Klyshko, the SPDC setup of Fig. 2 is equivalent to the layout shown here, for the case of a plane wave pump beam. Photons are "emitted" by the signal detector through the signal path, reflected by a mirror whose properties depend on the pump-beam parameters, and are finally detected in the idler path. The lenses L_s and L_i are placed so that they image the two SPP planes onto each other.

thus yielding

$$|j\rangle_i = \sum_{l;p;p^0} C_{l;p;p^0} h_{\frac{1}{2}}^{(n)}(0) |j\rangle_l h_{\frac{1}{2}}^{(m)}(0) |p^0\rangle_i \quad (16)$$

We now continue to calculate the coincidence fringe that is expected in the proposed experiment. In the signal path we place an analyzer consisting of a SPP with $\ell = j + \frac{1}{2}$ where j is an integer, with its orientation set to $\ell' = 0$, represented by $\hat{S}^y(0; j + \frac{1}{2})$, and a single-mode fiber. When the detector clicks, the signal state before passing through this analyzer is collapsed to $\hat{S}^y(0; j + \frac{1}{2}) |j\rangle_i = |j\rangle_i h_{\frac{1}{2}}^{(j)}(0)$.

When assuming half-integer OAM conservation per measurement, we would expect that detection of a signal photon in the state $\hat{S}^y(0; j + \frac{1}{2}) |j\rangle_i = |j\rangle_i h_{\frac{1}{2}}^{(j)}(0)$ collapses the idler photon to the state $\hat{S}^y(0; j + \frac{1}{2}) |j\rangle_i = |j\rangle_i h_{\frac{1}{2}}^{(j)}(0)$. Then, when rotating the idler SPP, we would expect to observe a parabolic coincidence fringe identical to that of Fig. 4 (aside from a scaling factor). The condition for this conservation to hold per measurement, is given by $n = m - 1$ in Eq. (16); in that case the OAM of the signal and idler photon equals $m + \frac{1}{2}$ (in units of \sim) and $m - 1 + \frac{1}{2} = m - \frac{1}{2}$, respectively, yielding

$$|j\rangle_i = \sum_{m;l;p;p^0} C_{m;l;p;p^0} h_{\frac{1}{2}}^{(m-1)}(0) |j\rangle_l h_{\frac{1}{2}}^{(m)}(0) |p^0\rangle_i \quad (17)$$

with $C_{m;l;p;p^0} = C_{l;p;p^0} h_{\frac{1}{2}}^{(m-1)}(0) |j\rangle_l h_{\frac{1}{2}}^{(m)}(0) |p^0\rangle_i$. How-

ever, m and n in Eq. (16) can take on any integer value and so half-integer OAM is not necessarily conserved per measurement. Although the phase-matching relations in the non-linear optical process enforce conservation of integer OAM, as expressed in Eq. (14) and leading to Eq. (16), they do not lead, apparently, to conservation of half-integer OAM per measurement. The terms in Eq. (16) with $n \notin m + 1$ are apparently essential, hence we have to use Eq. (16) instead of Eq. (17).

We now pose the question whether the parabolic coincidence fringe "derived" above survives the fact that half-integer OAM is not necessarily conserved per measurement. We therefore place in the idler path an analyzer that is complementary to the SPP in the signal beam at an orientation θ , i.e. the SPP is represented by $\hat{S}^Y(\theta; j + \frac{1}{2}) = \hat{S}^X(\theta; j - \frac{1}{2})$. When considering the two-photon state given of Eq. (14), the probability amplitude for both detectors ring in coincidence is given by

$$B_j(\theta) = \sum_{l, p, p^0}^X C_{l, p, p^0} h_{00}^j |p\rangle \langle i | h_{00}^j |p^0\rangle \langle i | \quad (18)$$

$$h_{\frac{1}{2}}^{j+1}(\theta) |j\rangle \langle i | h_{\frac{1}{2}}^j(\theta) |j\rangle \langle i |$$

Note that, as we neglect propagation of the emitted photons between the crystal and the SPPs, we implicitly assume that in Fig. 5, the lenses L_s and L_i not only image the two SPP planes onto each other, but also image the crystal plane onto each SPP plane. We rewrite Eq. (18), introducing a new relative weight constant,

$$C_1 = \sum_{p, p^0=0}^X C_{l, p, p^0} h_{00}^j |p\rangle \langle i | h_{00}^j |p^0\rangle \langle i | \quad (19)$$

so that

$$B_j(\theta) = \frac{1}{2^2} \sum_{l=1}^X C_1 \frac{\exp(i l \theta)}{(l + j + \frac{1}{2})^2} \quad (20)$$

As it is not possible to calculate the coefficients C_1 analytically, we use a numerical approach. When summing over p and p^0 in Eq. (19) from 0 to N (with N large), we find that C_1 behaves like a Gaussian as a function of l . When N increases, the width at half maximum of the Gaussian increases, but the height C remains the same. The width does not converge with increasing N , but instead increases with N , with $\frac{dN}{dl} = 0.55 \pm 0.01$. As N goes to infinity, the width of the Gaussian will also go to infinity and C_1 becomes equal to the constant C , i.e. independent of l . The resulting expression can be written as

$$B_j(\theta) = \frac{C}{2^2} \sum_{l=1}^X \frac{\exp(i l \theta)}{(l + j + \frac{1}{2})^2} \quad (21a)$$

$$= \exp\left(i \frac{1}{2} \theta + j \theta\right) b_e\left(\frac{\theta}{2}\right); \quad (21b)$$

where the summation in Eq. (21a) is, aside from a phase factor, equal to the Fourier expansion of the symmetric triangle function $b_e(\frac{\theta}{2})$, of which one period can be

written as

$$b_e(x) = \begin{cases} \frac{C}{2} \left(1 + \frac{2x}{\pi}\right); & -\frac{\pi}{2} < x < 0; \\ \frac{C}{2} \left(1 - \frac{2x}{\pi}\right); & 0 < x < \frac{\pi}{2}; \end{cases} \quad (22)$$

over a range of its argument x from $-\frac{\pi}{2}$ to $\frac{\pi}{2}$. We then find that the probability that both detectors ring in coincidence,

$$\mathcal{P}_j(\theta)^2 = \exp\left(i \frac{1}{2} \theta + j \theta\right) b_e\left(\frac{\theta}{2}\right)^2$$

$$= \frac{C^2}{4} \left(1 - \frac{2x}{\pi}\right)^2; \quad (23)$$

where $2 \in [0; 2\pi)$. So we find that the parabolic coincidence fringe survives.

Following the earlier reasoning that the parabolic overlap would be expected if half-integer OAM was conserved, and considering that the coincidence fringe remains parabolic, one may be inclined to believe that half-integer OAM is conserved per measurement. This is not the case. The fact that, after projection to two fundamental Gaussian modes by the single-mode fibers, the two-photon state in Eq. (16) and that in Eq. (17) yield the same result does not imply that they are the same. Namely, in the act of projection by the single-mode fibers, information is lost and only the contribution of the fundamental Gaussian to the signal and idler state survives. Thus, the equality of the true coincidence fringe and the artificial one (i.e. for the case where conservation is assumed), implies that the contribution of the fundamental LG state for both signal and idler together is the same in the two cases. It remains an open question whether the fact that the parabolic fringe survives the absence of a half-integer OAM conservation law has a deeper physical reason.

The above reasoning to obtain the coincidence fringe $\mathcal{P}_j(\theta)^2$ is valid for any choice of the signal SPP orientation and only depends on the relative orientation of the signal and idler SPPs. Thus a coincidence measurement on entangled OAM pairs using half-integer OAM analyzers, will bring forth a coincidence fringe that is parabolic, regardless of the individual settings of the analyzers.

VII. THE CHSH VERSION OF THE BELL INEQUALITY

There have been several theoretical papers that address the generalization of the Bell inequality [20] to quantify the violation of local realism of two N -dimensional particles (quN its) [3, 21, 22, 23, 24, 25]; an example of a quN it is a spin- s particle with $2s + 1 = N$. It has been pointed out that in this case the use of m_s -sorting devices, such as Stern-Gerlach analyzers, does not offer access to higher-dimensional quantum correlations, presumably because the action of a Stern-Gerlach analyzer depends only on the alignment of its quantization axis [23]. Instead of larger spin values ($s > \frac{1}{2}$), the use

of spatial degrees of freedom together with Bell multiports has been advocated to gain access to the multidimensional aspects of entanglement [23]. We stress that all this is different from our proposed use of half-integer SPPs ($s + \frac{1}{2}$). These devices do not produce finite- N qubits, but imprint the infinite OAM dimensionality of the (oriented) edge on a transmitted light field. Rotation of this edge is equivalent to a partial exploration of the complete Hilbert space along a certain path, namely an iso-OAM path; due to this complexity, it is not clear how a generalized Bell inequality could be applied to our case.

However, instead of using a generalized high-dimensional bipartite Bell inequality, it is allowed to use an inequality for lower-dimensional two-particle entanglement [25]. Thus we choose, as in the polarization case, the inequality introduced by Clauser, Horne, Shimony and Holt (CHSH) for a measurement where the coincidence probability is expected to be a function of only s and i [26]. When relabelling s and i as 1 and 2 (in no particular order), the CHSH inequality is given by [8, 27]

$$S = E(x_1; y_2) - E(x_1^0; y_2) + E(x_1; y_2^0) + E(x_1^0; y_2^0) \quad (24)$$

The function E is specified, for the variables $x; y$, as [8, 28]

$$E(x; y) = \frac{P(x; y) + P(x^2; y^2) - P(x; y^2) - P(x^2; y)}{P(x; y) + P(x^2; y^2) + P(x; y^2) + P(x^2; y)} \quad (25)$$

The notation x^2 (and similarly for y^2) is used to indicate an analyzer setting that analyses a state orthogonal to the state with setting x . Thus in our case, $x^2 = x + \pi$ and $y^2 = y + \pi$. $P(x; y)$ is the coincidence probability function, which is equal to

$$P(x; y) = b_e \frac{y - xj}{2}^2 = \frac{C^2}{4} [1 - \frac{y - xj}{2}]^2 \quad (26)$$

As the periodicity in the present case is half that of the case of polarization entanglement, we use the standard analyzer settings for polarization entanglement [8, 29] multiplied by a factor of two: $x_1 = \frac{1}{4}$, $x_1^0 = \frac{3}{4}$, $x_2 = \frac{1}{2}$, $x_2^0 = 0$.

Substitution yields a Bell parameter $S = 3\frac{1}{5}$. This is the key result of our paper; it indicates that in the case of entanglement of half-integer OAM states, the maximum violation of the CHSH inequality, given by Eq. (24), is stronger than the maximum violation that is allowed in polarization entanglement, namely $S = 2\sqrt{2}$. In other words, quantum non-locality of the photons in the proposed setup is stronger than the maximum achievable for

two qubits. To achieve this, only two detectors are required and only one coincidence count rate is measured per analyzer setting, in contrast to the OAM qubit setup requiring N detectors and N^2 coincidence count rates per analyzer setting [3, 23].

VIII. CONCLUSIONS

In this paper we have put forward a novel approach to demonstrate high-dimensional entanglement of orbital angular momentum states. The proposed setup uses analyzers that consist of non-integer SPPs and single-mode fibers, enabling detection of high-dimensional entanglement with only two detectors. The theoretical framework that we use is the advanced-wave theory of Klyshko et al., [13].

The key idea is to use the orientation of the edge dislocation in the SPPs. We specialize to the case of half-integer ℓ , so that the orientation of the edge as an analyzer setting can, to a certain extent, be treated similarly as the axis of a polarizer in polarization entanglement. Instead of horizontal and vertical polarization states, we deal with 'up' and 'down' states, referring to the orientation of the edge dislocation. To this end, we have described the orbital angular momentum states in a new basis and found that in SPDC, the two-photon state written in this basis does not show conservation of half-integer OAM. We use a mixed analytical-numerical approach to calculate the coincidence fringe in the entanglement setup and find it to be parabolic in shape, and periodic over 2π . When evaluating the well-known CHSH Bell parameter, we find $S = 3\frac{1}{5}$, i.e. we predict beyond-Bell pairing of two photons. To achieve this, we require only two detectors, as opposed to the standard multiport approach [3, 23]. This economic exploitation of the spatial degrees of freedom seems to be a consequence of the singular nature of our half-integer SPPs, which implies, in principle, infinite dimensionality.

Experimental verification of the outlined proposal is underway.

Acknowledgements

We acknowledge M. P. van Exter for fruitful discussions regarding the CHSH version of the Bell inequality. This work is part of the research program of the 'Stichting voor Fundamenteel Onderzoek der Materie (FOM)' and is supported by the EU programme ATESIT.

[1] L. Allen, M. W. Beijersbergen, R. J. C. Spreeuw, and J. P. Woerdman, Phys. Rev. A 45, 8185 (1992).

[2] A. Mair, A. Vaziri, G. Weihs, and A. Zeilinger, Nature

- 412, 313 (2001).
- [3] A. Vaziri, G. Weihs, and A. Zeilinger, *Phys. Rev. Lett.* 89, 240401 (2002).
- [4] J. P. Reskill, *Phys. Today* 52, 24 (1999).
- [5] G. F. Brand, *Amer. J. Phys.* 67, 55 (1999).
- [6] I. Basisti, V. Y. Bazhenov, M. S. Soskin, and M. V. Vasnetsov, *Opt. Commun.* 103, 422 (1993).
- [7] M. W. Beijersbergen, R. P. C. Coerwinkel, M. K. Kristensen, and J. P. Woerdman, *Opt. Commun.* 112, 321 (1994).
- [8] P. G. Kwiat, K. Mattle, H. Weinfurter, and A. Zeilinger, *Phys. Rev. Lett.* 75, 4337 (1995).
- [9] S. J. van Enk and G. Nienhuis, *Opt. Commun.* 94, 147 (1992).
- [10] M. Abramowitz and I. A. Stegun, eds., *Handbook of mathematical functions* (Dover, New York, 1965).
- [11] N. R. Heckenberg, R. McDuff, C. Smith, H. Rubinsztein-Dunlop, and M. J. Wegener, *Opt. Quant. Elec.* 24, 5951 (1992).
- [12] There do exist holograms that can generate mixed screw-edge dislocations in optical fields, thus modifying the OAM expectation value by non-integer numbers. See for these holograms, M. V. Vasnetsov, I. V. Basisti and M. S. Soskin, in *International conference on singular optics*, (ed. M. S. Soskin) (SPIE-International Society for Optical Engineering, Bellingham, WA, 1998), vol. 3487 of *SPIE Proceedings*, pp. 29-33.
- [13] A. V. Belinskii and D. N. Klyshko, *Sov. Phys. JETP* 78, 259 (1994).
- [14] H. H. A. Maat and G. A. Barbosa, *Phys. Rev. Lett.* 85, 286 (2000).
- [15] E. R. Eliel, S. M. Dutra, G. Nienhuis, and J. P. Woerdman, *Phys. Rev. Lett.* 86, 5208 (2001).
- [16] H. H. A. Maat and G. A. Barbosa, *Phys. Rev. Lett.* 86, 5209 (2001).
- [17] S. Franke-Arnold, S. M. Barnett, M. J. Padgett, and L. Allen, *Phys. Rev. A* 65, 033823 (2002).
- [18] G. A. Barbosa and H. H. A. Maat, *Phys. Rev. A* 65, 053801 (2002).
- [19] J. P. Torres, Y. Deyanova, L. Tomer, and G. Molina-Terriza, *Phys. Rev. A* 67, 052313 (2003).
- [20] J. Bell, *Physics* 1, 195 (1964).
- [21] N. D. Mermin, *Phys. Rev. D* 22, 356 (1980).
- [22] A. Peres, *Phys. Rev. A* 46, 4413 (1992).
- [23] D. Kaszlikowski, P. Gnaniński, M. Żukowski, W. Mikaszewski, and A. Zeilinger, *Phys. Rev. Lett.* 85, 4418 (2000).
- [24] T. Durt, D. Kaszlikowski, and M. Żukowski, *Phys. Rev. A* 64, 024101 (2001).
- [25] D. Collins, N. Gisin, N. Linden, S. Massar, and S. Popescu, *Phys. Rev. Lett.* 88, 040404 (2002).
- [26] J. F. Clauser, M. A. Home, A. Shimony, and R. A. Holt, *Phys. Rev. Lett.* 23, 880 (1969).
- [27] A. Peres, *Quantum theory: concepts and methods* (Kluwer Academic Publishers, Dordrecht, 1993).
- [28] A. G. Aruocchio and V. A. Rapisarda, *Nuovo Cimento* 65, 269 (1981).
- [29] J. F. Clauser and M. A. Home, *Phys. Rev. D* 10, 526 (1974).